

Finite-Time Teleportation Phase Transition in Random Quantum Circuits

Yimu Bao¹, Maxwell Block¹, and Ehud Altman^{1,2}

¹*Department of Physics, University of California, Berkeley, California 94720, USA*

²*Materials Sciences Division, Lawrence Berkeley National Laboratory, Berkeley, California 94720, USA*



(Received 30 October 2021; accepted 19 December 2023; published 19 January 2024)

How long does it take to entangle two distant qubits in a quantum circuit evolved by generic unitary dynamics? We show that if the time evolution is followed by measurements of all but two infinitely separated test qubits, then the entanglement between them can undergo a phase transition and become nonzero at a finite critical time t_c . The fidelity of teleporting a quantum state from an input qubit to an infinitely distant output qubit shows the same critical onset. Specifically, these finite-time transitions occur in short-range interacting two-dimensional random unitary circuits and in sufficiently long-range interacting one-dimensional circuits. The phase transition is understood by mapping the random continuous-time evolution to a finite-temperature thermal state of an effective spin Hamiltonian, where the inverse temperature equals the evolution time in the circuit. In this framework, the entanglement between two distant qubits at times $t > t_c$ corresponds to the emergence of long-range ferromagnetic spin correlations below the critical temperature. We verify these predictions using numerical simulation of Clifford circuits and propose potential realizations in existing platforms for quantum simulation.

DOI: [10.1103/PhysRevLett.132.030401](https://doi.org/10.1103/PhysRevLett.132.030401)

The dynamics of entanglement in many-body quantum systems is the focus of intense theoretical [1–4] and experimental interest [5–8]; indeed, it provides crucial insights for understanding the capacity of physical systems to process quantum information as well as the computational complexity involved in simulating their dynamics [9]. In generic unitary evolution with short-range interactions, the Lieb-Robinson bound [10] ensures that quantum entanglement propagates along light cones. Thus, 2 degrees of freedom separated by a distance L take a time of order L to get entangled.

Entanglement can be created much faster by supplementing unitary evolution with measurements [11–13]. As a simple example, we consider a chain of qubits initialized in a product of Bell pairs on the *odd* links, which can be prepared from a product state by a single layer of 2-qubit gates. By performing Bell measurements on the *even* links, one can create a Bell pair of the (unmeasured) first and last qubit. As another example, a two-dimensional cluster state can be used for measurement-based quantum computation [14]; one can create any desired entangled state by appropriate local measurements.

In the schemes described above, entanglement is generated over arbitrarily long distances using a unitary circuit of constant depth followed by a single layer of measurements. These states are said to possess finite localizable entanglement for two distant qubits (hence infinite entanglement length) [15,16]. However, the examples above are highly fine-tuned. It is natural to ask how long it would take to create quantum correlations between distant qubits using generic unitary evolution followed by local measurements.

In this Letter, we show that the creation of states with infinite entanglement length can occur as a phase transition at a critical time of order one. In the simplest setup, an initial product state is evolved for a time t , after which all but two infinitely separated qubits are measured. In two (or higher) dimensional systems with short-range interactions, entanglement between the two distant qubits onsets at a critical time t_c . The same is true for one-dimensional systems with sufficiently long-range interactions. An equivalent scheme, shown in Fig. 1(a), is to consider the teleportation from an input qubit to an infinitely distant output qubit after measuring all other output qubits, which can be achieved with nonvanishing fidelity after time t_c .

We provide a theoretical picture of this transition by mapping the random circuit evolution to an effective equilibrium problem. This approach builds on recent developments in describing entanglement dynamics through mapping circuits consisting of random unitaries to the statistical mechanics of classical spins located at the space-time positions where the gates operate [17–21]. In the case of continuous-time evolution, the classical spin model can be viewed as imaginary time evolution generated by an effective quantum Hamiltonian [22,23].

Previously, this mapping was primarily applied to understand the steady-state entanglement properties, which are determined by the ground state of the effective Hamiltonian (i.e., infinite imaginary time evolution). Similarly, the finite-time evolution, which we consider here, is related to a thermal state of the effective Hamiltonian (i.e., finite imaginary time evolution). The key point is that a

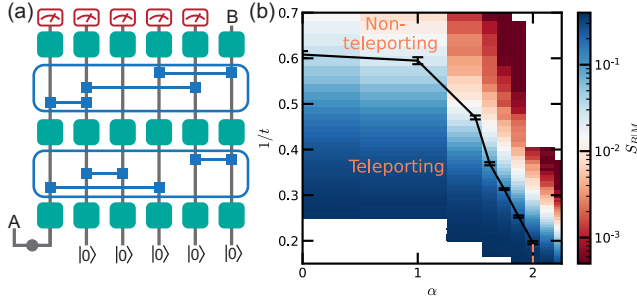


FIG. 1. (a) Random quantum circuit on N qubits. In each time step δt , we apply single-qubit Haar-random gates to every qubit followed by $N\delta t$ 2-qubit Haar-random gates. The distribution of 2-qubit gates is determined by the geometry of the circuit. Initially, the first qubit is maximally entangled with a reference qubit A , while the remaining qubits are prepared in $|0\rangle$. We consider the entropy of an output qubit B conditioned on local measurements on the rest of the qubits. (b) Phase diagram of one-dimensional long-range unitary circuits with power-law decaying interaction. The black markers represent the inverse critical time $1/t_c$ as a function of power-law exponent α . The transition exists for $\alpha \leq 2$, indicated by the pink dashed line. The color indicates the conditional entropy $S_{B|M}$.

finite-temperature transition in the thermal state indicates a finite real-time transition in the circuit.

We demonstrate this phenomenon by considering the transition in continuous-time random unitary circuits (RUC) with different architectures including two-dimensional short-range systems, all-to-all coupled systems, and one-dimensional long-range systems with power-law decaying interactions. In the last case, our theory predicts a finite-time transition for power-law exponent $\alpha \leq 2$, and specifically a Kosterlitz-Thouless- (KT) like transition at $\alpha = 2$. We corroborate these predictions with numerical simulations of random Clifford circuits.

Before proceeding, we remark on a related paper by Napp *et al.* [24] dealing with the sampling complexity of shallow two-dimensional brick-layer RUCs. This work claimed and provided evidence that approximate sampling from such circuits is hard if the depth t is above a threshold t_c of $O(1)$ while it is easy for $t < t_c$. Sampling requires measuring all qubits following the final layer of unitary gates. The essence of the argument is that this network can be contracted sideways, showing it is equivalent to simulating the dynamics of a one-dimensional quantum circuit with measurements. Hence, one expects a phase transition in sampling complexity in shallow two-dimensional RUCs which is of the same universality as the measurement-induced transition in one dimension [3,4,25–27]. In our discussion, we argue heuristically that this sampling transition can be understood as a specific example of the teleportation transition, and may therefore occur in a broad class of systems for which the effective Hamiltonian exhibits a finite-temperature transition.

Setup and theoretical framework.—Our model consists of N qubits with $N - 1$ qubits initialized in a product state and a single qubit prepared in a maximally entangled state with the reference A . In each time step δt , we apply a layer of single-qubit Haar-random unitary gates followed by $N\delta t$ 2-qubit Haar-random unitary gates [Fig. 1(a)]. The sites (i, j) on which each 2-qubit gate operates are drawn independently from a distribution $P(i, j)$, which depends on the specific models we discuss below. The single-qubit gates do not generate entanglement and are introduced only for analytical convenience [28]. After evolving for time t , we measure all $N - 1$ qubits except for a distant qubit B .

The resulting fidelity of teleportation between qubits A and B can be quantified (without considering an explicit decoding scheme) by the entanglement entropy of B , conditioned on the measurement outcomes of qubits M [29]. To analytically determine the conditional entropy $S_{B|M}$ averaged over circuit realizations and measurement outcomes, we formulate it as the $n \rightarrow 1$ limit (replica limit) of the quantities [20],

$$S_{B|M}^{(n)} = \frac{1}{1-n} \log \frac{\overline{\sum_m \text{tr} \tilde{\rho}_{B,m}^n}}{\sum_m \text{tr} \tilde{\rho}_m^n}, \quad (1)$$

where $\tilde{\rho}_m := \hat{P}_m \rho \hat{P}_m$ is the projection of the density matrix onto the set of measurement outcomes labeled by m , and the overline indicates the average over the Haar ensemble. Accordingly, the probability for this set of measurement outcomes is $p_m = \text{tr}(\rho \hat{P}_m) = \text{tr} \tilde{\rho}_m$, and the normalized density matrix is $\rho_m = \tilde{\rho}_m / p_m$. We note that the $S_{B|M}^{(n)}$ are not precisely the conditional Rényi entropies because the average is taken inside the logarithm.

The simplest quantity that captures the qualitative features of $S_{B|M}$ is $S_{B|M}^{(2)}$, although the critical exponents of their respective transitions may be different [19–21]. The quantity $S_{B|M}^{(2)}$ involves the second moments of the density matrix, which can be determined from the double density matrix $\rho \otimes \rho$. Formally, $\rho \otimes \rho$ can be represented as a state vector $|\rho\rangle\rangle$ in the replicated Hilbert space $\mathcal{H}^{(2)} := (\mathcal{H} \otimes \mathcal{H}^*)^{\otimes 2}$, where \mathcal{H} (\mathcal{H}^*) denotes the ket (bra) Hilbert space. A unitary gate U in the circuit acts as $\mathcal{U} = (U \otimes U^*)^{\otimes 2}$ on $|\rho\rangle\rangle$. Hence, the replicated density matrix undergoes unitary evolution $|\rho(t)\rangle\rangle = \prod_{\tau=1}^t \mathcal{U}_{2,\tau} \mathcal{U}_{1,\tau} |\rho(0)\rangle\rangle$, where $\mathcal{U}_{1,\tau}$ and $\mathcal{U}_{2,\tau}$ denote the layer of single- and 2-qubit gates in each time step τ , respectively.

The average dynamics of the double density matrix can be analytically mapped to imaginary time evolution under an effective Hamiltonian [22,23]. First, the average over single-qubit gates effects a projection from a 16-dimensional local Hilbert space to the two-dimensional Hilbert space of a spin-1/2 [29]. Then, the layer of 2-qubit gates reduces to a transfer matrix for the transition

amplitude between the spin-1/2 configurations in consecutive time steps, $\mathcal{T} = \mathbb{1} + N\delta t \sum_{ij} P(i, j) \overline{\mathcal{U}}_{2,\tau}(i, j)$.

The transfer matrix \mathcal{T} can be viewed as the infinitesimal imaginary time evolution generated by an effective quantum Hamiltonian operating on spin-1/2 degrees of freedom, $\mathcal{T} = e^{-\delta t H_{\text{eff}}}$. For our circuit, the effective Hamiltonian takes the form

$$H_{\text{eff}} = \sum_{i,j} J_{ij} \left[-\frac{2}{5} \sigma_i^z \sigma_j^z - \frac{1}{10} \sigma_i^y \sigma_j^y - \frac{1}{5} (\sigma_i^x + \sigma_j^x) \right], \quad (2)$$

where the coupling $J_{ij} = NP(i, j)$ is given by the average number of 2-qubit gates acting between qubit i and j in every unit time [33]. Accordingly, the replicated, unnormalized, density matrix evolves as $|\rho(t)\rangle\rangle = e^{-tH_{\text{eff}}} |\rho(0)\rangle\rangle$. We note that the Hamiltonian exhibits a global Ising symmetry generated by $\prod_i \sigma_i^z$, which stems from the invariance of \mathcal{U} under the permutation of two copies of ket (or bra) Hilbert space.

The effective imaginary time evolution above yields a thermal state of the ferromagnetic Ising Hamiltonian in Eq. (2) at inverse temperature t . For two-dimensional RUCs, the associated two-dimensional Ising model will undergo a ferromagnetic transition at a temperature corresponding to a finite critical time t_c . Similarly, for one-dimensional RUCs, the associated one-dimensional Ising model can exhibit a finite-temperature transition provided the unitary couplings decay with a sufficiently small power of distance $\alpha \leq 2$ [34–37]. This finite-temperature phase transition implies a transition in the output state of the circuit occurring at a finite time.

This transition manifests in the conditional entropy $S_{B|M}^{(2)}$. The projective measurements of the output state play a crucial role in revealing the transition: they impose a boundary condition in the finite imaginary time evolution that preserves the Ising symmetry [20,21]. In more detail, $S_{B|M}^{(2)}$ is mapped to the excess free energy associated with imposing symmetry-breaking fields only at the space-time locations of qubit A and B . This can be further reduced to the imaginary time order parameter correlation function, $S_{B|M}^{(2)} \sim \langle \sigma_B^z(t) \sigma_A^z(0) \rangle$ [29]. Consequently, $S_{B|M}^{(2)}$ is nondecaying in the ordered phase ($t > t_c$) due to the long-range order in the Ising model, whereas $S_{B|M}^{(2)}$ rapidly decays to zero in the disordered phase ($t < t_c$).

We remark that there is no finite-time transition in the purity or entanglement entropy of an extensive subsystem in the output state. In the effective spin model, such quantities involve a symmetry-breaking field at the final time [17–19]. Since we are concerned with spontaneous symmetry breaking in the slab, whose thickness is the evolution time of order one, the symmetry-breaking fields necessarily eliminate the transition.

Examples and numerical results.—We demonstrate the finite-time teleportation transition predicted above in three exemplary models: (1) all-to-all interacting quantum circuits, (2) one-dimensional quantum circuits with power-law decaying long-range interactions, and (3) two-dimensional quantum circuits with short-range interactions. To verify our theoretical predictions, we compute the conditional entropy in random Clifford circuits, which can be efficiently simulated [38,39]. Although Clifford circuits, which only form a unitary 3-design [40], are not the same as Haar-random circuits, they still exhibit a finite-time transition with the same qualitative behavior.

First, we consider the circuit with all-to-all unitary gates. Within a time step δt , each 2-qubit gate is drawn independently and operates on a random pair of qubits (i, j) with equal probability. Hence, the effective quantum Hamiltonian that describes $S_{B|M}^{(2)}$ has all-to-all couplings $J_{ij} \sim 1/N$ [29]. In the limit $N \rightarrow \infty$, the Ising phase transition in this Hamiltonian is described exactly by mean-field theory, which predicts critical exponents $\nu_{\text{MF}} = 2$, $\beta_{\text{MF}} = 0.5$, and a critical time $t_c^{(2)} = 2.0$ [29]. We note that the mean-field theory does not yield a reliable t_c for $S_{B|M}$ as the effective Hamiltonian is derived for an approximate quantity $S_{B|M}^{(2)}$.

To characterize the transition of the conditional entropy $S_{B|M}$, we simulate this quantity in all-to-all Clifford circuits of system sizes up to $N = 512$ as shown in Fig. 2(a) [41,42]. We perform a finite-size scaling analysis based on the scaling formula for order parameter correlation function to extract critical exponents [29]:

$$S_{B|M}(t, N) = N^{-2\beta/\nu} \mathcal{F}((t - t_c)N^{1/\nu}). \quad (3)$$

This analysis yields critical exponents $\nu = 2.1 \pm 0.2$, $\beta = 0.4 \pm 0.1$, which are in close agreement with the predictions of the mean-field theory, and also the critical time $t_c \approx 1.6$.

Next, we consider a one-dimensional array of N qubits evolving with power-law decaying couplings and periodic boundary conditions. Here, for each 2-qubit gate, we independently choose a random pair of sites (i, j) with a probability $P(i, j) \propto 1/|i - j|^\alpha$. The effective model for this circuit is a one-dimensional finite-width classical Ising model with long-range coupling $J_{ij} \sim 1/|i - j|^\alpha$.

This model is in the same universality class as the one-dimensional long-range classical Ising chain at finite temperature, which has been extensively studied and shown to have an ordering transition when $\alpha \leq 2$ [34–37], with KT universality at $\alpha = 2$ [43–48]. Furthermore, for $3/2 < \alpha < 2$, the transition features continuously varying critical exponents, whereas for $\alpha \leq 3/2$, it is described by mean-field theory with α -independent exponents [43].

These predictions from the classical Ising chain are borne out clearly in our Clifford numerics. For $\alpha \leq 2$,

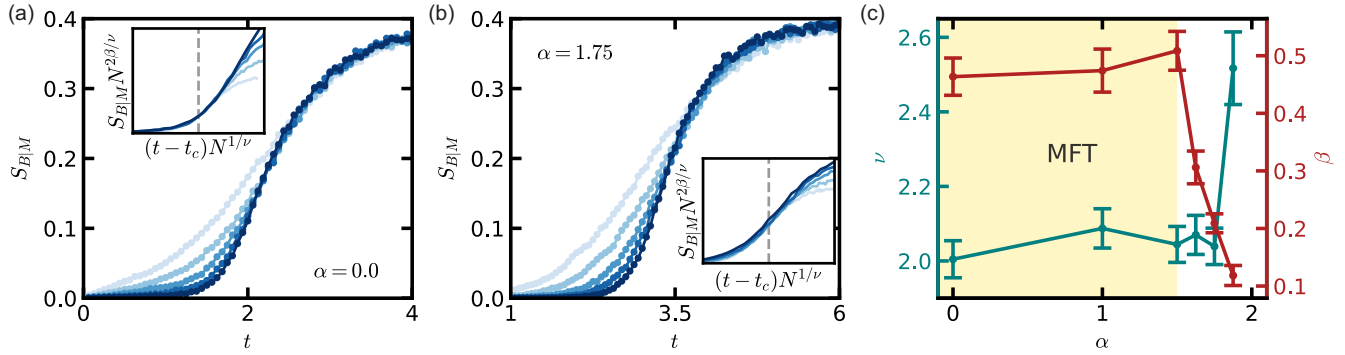


FIG. 2. Finite-time transition in one-dimensional long-range interacting random circuits. (a),(b) The conditional entropy $S_{B|M}$ in circuits with power-law exponents $\alpha = 0$ [all-to-all (a)] and $\alpha = 1.75$ [(b)] plotted as a function of time t for various system sizes N from 32 to 512 indicated by increasing opacity. Inset: finite-size scaling collapse using Eq. (3). The gray dotted line indicates t_c . For the all-to-all circuit ($\alpha = 0$), we obtain critical exponents $\nu \approx 2.0$, $\beta \approx 0.46$, and critical time $t_c \approx 1.6$. For $\alpha = 1.75$, we obtain $\nu \approx 2.0$, $\beta \approx 0.20$, and critical time $t_c \approx 2.1$. (c) Critical exponents ν and β for $\alpha < 2$. The exponents for $\alpha \leq 1.5$ agree with the prediction from mean-field theory (MFT). Moreover, near $\alpha = 2$, ν begins to diverge, as expected near a KT-like transition. The finite-time transition does not exist for $\alpha > 2$. The numerical results are averaged over 1.5×10^4 random circuit realizations.

we simulate $S_{B|M}$ for A and B separated by $N/2$ sites and observe a crossing for various N , as exemplified at $\alpha = 1.75$ in Fig. 2(b) [29]. We perform the finite-size scaling to determine the exponents [summarized in Fig. 2(c)] [49]. On the other hand, we do not observe a finite-time transition in $S_{B|M}$ for $\alpha > 2$ [29]. A phase diagram is presented in Fig. 1(b).

The point $\alpha = 2$ requires special attention. Here, the effective model exhibits a finite-temperature KT transition, which does not admit single-parameter scaling as postulated in Eq. (3). The exponential divergence of the correlation length can be viewed as having $\nu \rightarrow \infty$. Indeed, Fig. 2(c) shows a sharp increase of ν upon approaching $\alpha = 2$. At $\alpha = 2$ we compare the observed scaling of $S_{B|M}(t, N)$ to the scaling form $a \exp[1/(\log N + b)]$ expected in an Ising chain with inverse square interaction [45]. We find an accurate fit at the critical time $t_c \approx 5.0$ [29], which supports a KT-like transition. However, simulations on larger system sizes are needed to precisely determine the universality of this transition.

Last, we consider the finite-time transition in short-range interacting circuits in higher dimensions ($d \geq 2$). Specifically, we consider $P(i, j)$ to be uniformly distributed over pairs of nearest-neighbor qubits. The critical exponents extracted from the two-dimensional Clifford simulation are $\nu \approx 1.2$, $\beta \approx 0.11$ [Fig. 3(b)]. These exponents agree with those found in the (1 + 1)D measurement-induced entanglement transition [50,51]. This result is indeed expected by mapping the dynamics of a finite depth two-dimensional brick-layer RUC with final-time measurements to monitored quantum dynamics in one dimension [24].

Discussion.—The above analysis of two-dimensional circuits suggests that the finite-time teleportation transition may generally correspond to a transition in approximate

sampling complexity [24,52]. Specifically, we consider the problem of sampling measurement outcomes from N qubits initialized in a product state and evolved under a finite-time RUC. To draw a connection to the teleportation transition, we divide the output qubits into three regions: \mathcal{A} and \mathcal{B} , each with a subextensive number of qubits N^γ with $0 < \gamma < 1$, and M , the remaining qubits.

In the teleporting phase ($t > t_c$), measurements on M generate long-range entanglement between subsystems \mathcal{A} and \mathcal{B} . In the spin model, $S_{B|M}$ is the excess free energy of imposing a domain wall separating \mathcal{A} from \mathcal{B} , which scales as a power law of $\min(|\mathcal{A}|, |\mathcal{B}|)$ in the ordered phase [53]. Thus, we expect approximate sampling from the pure joint state $|\psi_{\mathcal{A}\mathcal{B}}\rangle$ to be as complex as sampling from a

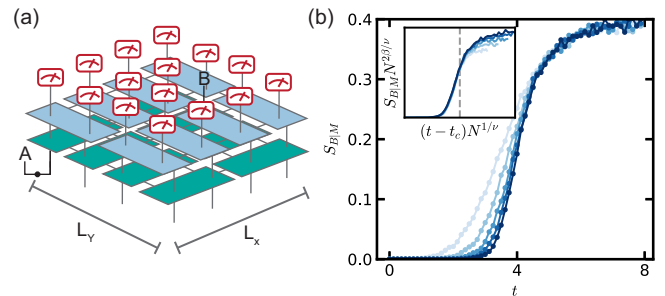


FIG. 3. Finite-time teleportation transition in two-dimensional short-range random circuits. (a) Schematic of a circuit of size $L_x = L_y = L$. We use periodic boundary conditions and consider reference A to be entangled with an input qubit separated from output qubit B by $L/2$ in both directions. (b) The conditional entropy $I_{B|M}$ plotted as a function of time t for L from 8 to 24 indicated by increasing opacity. Inset: finite-size scaling collapse using Eq. (3). We obtain $\nu \approx 1.2 \pm 0.1$, $\beta \approx 0.11 \pm 0.03$, and critical time $t_c \approx 4.2$ (indicated by the gray dashed line). The numerical results are averaged over 9000 random circuit realizations.

Haar-random state of a subextensive power-law number of qubits, which is believed to be classically hard [54].

On the other hand, in the nonteleporting phase ($t < t_c$), the effective model has a finite correlation length ξ ; i.e., sampling from a given qubit is independent from sufficiently distant qubits. Indeed, it has been shown for brick-layer circuits that approximate sampling can be achieved by patching simulations of subregions of size $O[(\log N)^d]$ together, resulting in a $\text{Poly}(N)$ run-time in two dimensions and quasi- $\text{Poly}(N)$ run-time in higher dimensions [24]. However, establishing a rigorous connection between finite-time teleportation in Haar-random circuits with arbitrary connectivity and sampling complexity remains an open question for future work.

Although 1D short-range RUCs do not feature a finite-time transition, the spin model mapping indicates an exponentially diverging correlation length $\xi \sim \exp(Jt)$ with circuit depth t . This results from the correlation length $\xi \sim \exp(J/T)$ in the 1D quantum Ising model at temperature T with coupling J . Therefore, one can teleport qubits over a distance N in circuits of depth $t \sim \log N$ [55].

The teleportation transition we describe can potentially be realized on leading quantum simulation platforms, such as trapped-ion systems, which feature tunable long-range interactions [57], and two-dimensional superconducting circuits [6,58,59]. We note, however, that obtaining the conditional entropy in experiments is challenging as naive evaluation of $S_{B|M}$ requires postselection on an extensive number of qubits. Alternatively, one can verify the entanglement by decoding from the output qubit, which is a topic of ongoing research for generic evolution beyond Clifford circuits [8,64].

Our framework is also applicable to studying finite-time transitions in other circuit ensembles. In circuits with conserved quantities, the effective Hamiltonian is governed by an enlarged symmetry allowing a richer phase structure at finite times [22]. For example, in free fermion dynamics that conserve fermion parity, the effective Hamiltonian exhibits a continuous $U(1)$ symmetry. In two dimensions, the effective model undergoes a finite-time KT transition and can support power-law decaying $S_{B|M}$, while in dimension $d \geq 3$, the continuous symmetry can be broken, leading to nondecaying $S_{B|M}$. Moreover, we note that the key dynamical feature that enables the teleportation transition is the protection of quantum information against local measurements. Thus, we conjecture that the transition can also occur in nonrandom chaotic Hamiltonian dynamics in which local scrambling protects information.

We thank Soonwon Choi, Abhinav Deshpande, Michael Gullans, Nishad Maskara, Norman Yao, and Xiaoliang Qi for useful discussions. We are grateful to Alex Dalzell for insightful feedback and carefully explaining the work of Ref. [24]. This material is based upon work supported by the U.S. Department of Energy, Office of Science, National

Quantum Information Science Research Centers, Quantum Systems Accelerator. This work was supported in part by the NSF QLCI program through Grant No. OMA-2016245. M. B. acknowledges support through the Department of Defense (DOD) through the National Defense Science and Engineering Graduate (NDSEG) Fellowship Program. E. A. acknowledges support from the Gyorgy Chair in Physics at UC Berkeley.

-
- [1] H. Kim and D. A. Huse, *Phys. Rev. Lett.* **111**, 127205 (2013).
 - [2] A. Nahum, J. Ruhman, S. Vijay, and J. Haah, *Phys. Rev. X* **7**, 031016 (2017).
 - [3] B. Skinner, J. Ruhman, and A. Nahum, *Phys. Rev. X* **9**, 031009 (2019).
 - [4] Y. Li, X. Chen, and M. P. A. Fisher, *Phys. Rev. B* **98**, 205136 (2018).
 - [5] A. M. Kaufman, M. E. Tai, A. Lukin, M. Rispoli, R. Schittko, P. M. Preiss, and M. Greiner, *Science* **353**, 794 (2016).
 - [6] F. Arute, K. Arya, R. Babbush, D. Bacon, J. C. Bardin, R. Barends, R. Biswas, S. Boixo, F. G. Brandao, D. A. Buell *et al.*, *Nature (London)* **574**, 505 (2019).
 - [7] J. Choi, A. L. Shaw, I. S. Madjarov, X. Xie, R. Finkelstein, J. P. Covey, J. S. Cotler, D. K. Mark, H.-Y. Huang, A. Kale *et al.*, *Nature (London)* **613**, 468 (2023).
 - [8] C. Noel, P. Niroula, D. Zhu, A. Risinger, L. Egan, D. Biswas, M. Cetina, A. V. Gorshkov, M. J. Gullans, D. A. Huse *et al.*, *Nat. Phys.* **18**, 760 (2022).
 - [9] G. Vidal, *Phys. Rev. Lett.* **91**, 147902 (2003).
 - [10] E. H. Lieb and D. W. Robinson, *Statistical Mechanics* (Springer, New York, 1972), pp. 425–431.
 - [11] H.-J. Briegel, W. Dür, J. I. Cirac, and P. Zoller, *Phys. Rev. Lett.* **81**, 5932 (1998).
 - [12] Y. Li, X. Chen, A. W. W. Ludwig, and M. P. A. Fisher, *Phys. Rev. B* **104**, 104305 (2021).
 - [13] J. S. Cotler, D. K. Mark, H.-Y. Huang, F. Hernandez, J. Choi, A. L. Shaw, M. Endres, and S. Choi, *PRX Quantum* **4**, 010311 (2023).
 - [14] R. Raussendorf and H. J. Briegel, *Phys. Rev. Lett.* **86**, 5188 (2001).
 - [15] F. Verstraete, M. Popp, and J. I. Cirac, *Phys. Rev. Lett.* **92**, 027901 (2004).
 - [16] M. Popp, F. Verstraete, M. A. Martín-Delgado, and J. I. Cirac, *Phys. Rev. A* **71**, 042306 (2005).
 - [17] P. Hayden, S. Nezami, X.-L. Qi, N. Thomas, M. Walter, and Z. Yang, *J. High Energy Phys.* **11** (2016) 009.
 - [18] A. Nahum, S. Vijay, and J. Haah, *Phys. Rev. X* **8**, 021014 (2018).
 - [19] R. Vasseur, A. C. Potter, Y.-Z. You, and A. W. W. Ludwig, *Phys. Rev. B* **100**, 134203 (2019).
 - [20] Y. Bao, S. Choi, and E. Altman, *Phys. Rev. B* **101**, 104301 (2020).
 - [21] C.-M. Jian, Y.-Z. You, R. Vasseur, and A. W. W. Ludwig, *Phys. Rev. B* **101**, 104302 (2020).
 - [22] Y. Bao, S. Choi, and E. Altman, *Ann. Phys. (Amsterdam)* **435**, 168618 (2021).

- [23] M. Block, Y. Bao, S. Choi, E. Altman, and N. Y. Yao, *Phys. Rev. Lett.* **128**, 010604 (2022).
- [24] J. C. Napp, R. L. La Placa, A. M. Dalzell, F. G. S. L. Brandao, and A. W. Harrow, *Phys. Rev. X* **12**, 021021 (2022).
- [25] Y. Li, X. Chen, and M. P. A. Fisher, *Phys. Rev. B* **100**, 134306 (2019).
- [26] S. Choi, Y. Bao, X.-L. Qi, and E. Altman, *Phys. Rev. Lett.* **125**, 030505 (2020).
- [27] M. J. Gullans and D. A. Huse, *Phys. Rev. X* **10**, 041020 (2020).
- [28] We note that single-qubit gate on site i can in principle change the circuit ensemble provided that no 2-qubit Haar-random gate acts on i .
- [29] See Supplemental Material at <http://link.aps.org/supplemental/10.1103/PhysRevLett.132.030401> for details, which includes Refs. [30–32].
- [30] J. Preskill, Lecture notes for physics 219: Quantum computation (2018).
- [31] B. Collins, *Int. Math. Res. Not.* **2003**, 953 (2003).
- [32] G. Yuval and P. Anderson, *Phys. Rev. B* **1**, 1522 (1970).
- [33] We note that because only N gates are applied per unit time, $\sum_{(i,j)} J_{ij} = N$, and therefore the energy of the Ising model is always extensive.
- [34] D. Ruelle, *Commun. Math. Phys.* **9**, 267 (1968).
- [35] F. J. Dyson, *Commun. Math. Phys.* **12**, 91 (1969).
- [36] D. Thouless, *Phys. Rev.* **187**, 732 (1969).
- [37] P. Anderson and G. Yuval, *J. Phys. C* **4**, 607 (1971).
- [38] D. Gottesman, [arXiv:quant-ph/9807006](https://arxiv.org/abs/quant-ph/9807006).
- [39] S. Aaronson and D. Gottesman, *Phys. Rev. A* **70**, 052328 (2004).
- [40] Z. Webb, *Quantum Inf. Comput.* **16**, 1379 (2016).
- [41] We ignore the single-qubit gates in the Clifford simulation as they do not affect the information dynamics.
- [42] We note that $S_{B|M}$ saturates to a maximum value 0.4 in the long time limit, which is universal for random Clifford evolution [13].
- [43] J. Kosterlitz, *Phys. Rev. Lett.* **37**, 1577 (1976).
- [44] J. L. Cardy, *J. Phys. A* **14**, 1407 (1981).
- [45] J. Bhattacharjee, S. Chakravarty, J. L. Richardson, and D. J. Scalapino, *Phys. Rev. B* **24**, 3862 (1981).
- [46] J. K. Bhattacharjee, J. L. Cardy, and D. J. Scalapino, *Phys. Rev. B* **25**, 1681 (1982).
- [47] J. Z. Imbrie and C. M. Newman, *Commun. Math. Phys.* **118**, 303 (1988).
- [48] E. Luijten and H. Meßingfeld, *Phys. Rev. Lett.* **86**, 5305 (2001).
- [49] For $\alpha \leq 3/2$ we find approximately constant critical exponents, consistent with mean-field theory. In contrast, for $3/2 < \alpha < 2$ we obtain continuously varying critical exponents.
- [50] A. Zabalo, M. J. Gullans, J. H. Wilson, S. Gopalakrishnan, D. A. Huse, and J. H. Pixley, *Phys. Rev. B* **101**, 060301(R) (2020).
- [51] The anomalous dimension in two dimensions is given by $\eta = 2\beta/\nu \approx 0.2$ in agreement with the result of [50].
- [52] N. Maskara, A. Deshpande, A. Ehrenberg, M. C. Tran, B. Fefferman, and A. V. Gorshkov, *Phys. Rev. Lett.* **129**, 150604 (2022).
- [53] The subextensive symmetry-breaking boundary conditions on \mathcal{A}, \mathcal{B} do not destroy the long-range order in the effective spin model.
- [54] A. Bouland, B. Fefferman, C. Nirkhe, and U. Vazirani, *Nat. Phys.* **15**, 159 (2019).
- [55] However, the approximate sampling from log N -depth 1D RUCs is tractable since $S_{B|M} = O(\log N)$ [56].
- [56] T. J. Osborne, *Phys. Rev. Lett.* **97**, 157202 (2006).
- [57] D. Porras and J. I. Cirac, *Phys. Rev. Lett.* **92**, 207901 (2004).
- [58] K. Satzinger, Y.-J. Liu, A. Smith, C. Knapp, M. Newman, C. Jones, Z. Chen, C. Quintana, X. Mi, A. Dunsworth *et al.*, *Science* **374**, 1237 (2021).
- [59] We remark that our protocol demonstrates a distinct teleportation mechanism from those inspired by quantum gravity [60–63], in which the teleportation distance is limited by the light cone of the evolution.
- [60] P. Hayden and J. Preskill, *J. High Energy Phys.* **09** (2007) 120.
- [61] K. A. Landsman, C. Figgatt, T. Schuster, N. M. Linke, B. Yoshida, N. Y. Yao, and C. Monroe, *Nature (London)* **567**, 61 (2019).
- [62] A. R. Brown, H. Gharibyan, S. Leichenauer, H. W. Lin, S. Nezami, G. Salton, L. Susskind, B. Swingle, and M. Walter, *PRX Quantum* **4**, 010320 (2023).
- [63] T. Schuster, B. Kobrin, P. Gao, I. Cong, E. T. Khabiboulline, N. M. Linke, M. D. Lukin, C. Monroe, B. Yoshida, and N. Y. Yao, *Phys. Rev. X* **12**, 031013 (2022).
- [64] M. J. Gullans and D. A. Huse, *Phys. Rev. Lett.* **125**, 070606 (2020).